Journal of Physics and Chemistry of Solids 72 (2011) 1430–1435

Contents lists available at SciVerse ScienceDirect

Journal of Physics and Chemistry of Solids

journal homepage: www.elsevier.com/locate/jpcs

Fabrication and characterization of ZnTPP:PCBM bulk heterojunction (BHJ) solar cells

S.M. Khan [a,b,*], M. Kaur [a], J.R. Heflin [a], M.H. Sayyad [b]

[a] Department of Physics, Virginia Polytechnic Institute and State University, Blacksburg, VA 24061, USA
[b] Faculty of Engineering Sciences, Ghulam Ishaq Khan Institute of Engineering Sciences and Technology, Topi, Khyber Pakhtunkhwa 23640, Pakistan

ARTICLE INFO

Article history:
Received 15 April 2011
Received in revised form
22 July 2011
Accepted 2 August 2011
Available online 6 September 2011

Keywords:
A. Fullerenes
A. Organic compounds
A. Thin films
B. Vapor deposition
C. Electron microscopy

ABSTRACT

Bulk heterojunction (BHJ) solar cells were fabricated based on blended films of a porphyrin derivative 5,10,15,20-Tetraphenyl-21H,23H-porphine zinc (ZnTPP) and a fullerene derivative [6,6]-phenyl-C_{61} butyric acid methyl ester (PCBM) as the active layer. The ZnTTP:PCBM BHJ solar cells were fabricated by spin-casting of the blended layer. The weight ratios of ZnTPP and PCBM were varied from 1:1 to 0:10. The electronic and optical properties of each cell were investigated. Optical density (*OD*) of the blended film for each cell was extracted from its reflection and transmission curves. OD and average absorption coefficients of the active materials were used to determine film thicknesses. Absorption spectra of each component material were compared with the spectra of the blended films. Current density–Voltage (*J–V*) characteristics were recorded under dark as well as under the illumination of AM 1.5G (1 sun) solar spectrum. The BHJ solar cell with ZnTPP:PCBM ratio of 1:9 showed the best performance . The values of *RR*, V_{OC} , J_{SC} , *FF* and η for these ratios were 106.3, 0.4 V, 1.316 mA/cm^2, 0.4 and 0.21%, respectively. The cross-section of this device using SEM was also examined.

1. Introduction

Organic photovoltaic (OPV) cells utilizing organic semiconductors have attracted considerable attention as next-generation solar cells from the viewpoint of light weight, flexibility and low-cost [1–3]. Fabrication of organic solar cells often involves relatively expensive techniques associated with vacuum evaporation or vapor deposition. Wet processes, such as spin coating and drop casting, have been recognized as low-cost, low-temperature and fast methods of obtaining organic thin films from solutions.

Some low molecular weight semiconductors demonstrate a high crystallinity and charge mobility through intermolecular interactions; however, they are inappropriate for wet processes because of their poor solubility in typical organic solvents and low quality film formation by wet processing. Therefore, OPV cells based on low molecular weight materials have been generally fabricated with layered [4,5] structures by thermal evaporation.

Photovoltaic devices with donor (D) and acceptor (A) species rely upon the diffusion of a photo-generated exciton to the nearest D–A interface, where it dissociates into an electron and a hole. Since the exciton diffusion distance is limited to <10 nm [5–7], it is therefore essential to control the composition of the electron donor and acceptor components on the nanometer length scale.

A simple, yet successful technique is the solution-processed bulk heterojunction (BHJ) solar cell. BHJ or blended devices, in which the semiconducting donor and acceptor are co-dissolved in an organic solvent and spin-coated as a single photoactive layer, provide good charge transfer from electron donor to acceptor. Hence, the main advantage of the bulk over the conventional (two layer) heterojunction is the large increase of the interfacial area between donor and acceptor moieties throughout the bulk volume of the film. Minimal loss due to too short exciton diffusion lengths is expected since excitons formed in a (perfect) bulk heterojunction are within reach of the D–A interface, which is dispersed throughout the bulk. Ideally, all excitons will be dissociated within their lifetime, giving rise to separated electrons and holes [8].

In the first report of solution processed BHJ solar cells, Yu et al. [1] used a highly soluble fullerene derivative, PCBM [9], to achieve sufficient percolation of charges through both components. Within the past few years, bulk heterojunctions utilizing small molecules have been reported. Table 1 summarizes some efforts to employ small molecules for BHJ solar cells fabricated both by wet and dry processing.

Porphyrins and phthalocyanine possess good thermal and photostabilities. They also exhibit some intriguing electrical and optical properties, so that there is a extensive research into their application in optical and optoelectronic devices such as photovoltaic cells, OLEDs and OFETs [15]. Porphyrins, macrocyclic aromatic compounds

* Corresponding author at: Faculty of Engineering Sciences, Ghulam Ishaq Khan Institute of Engineering Sciences and Technology, Topi, Khyber Pakhtunkhwa 23640, Pakistan. Tel.: +92 3335246035; fax: +92 938271890.
E-mail addresses: shahid938@hotmail.com, shahid938@yahoo.com (S.M. Khan).

0022-3697/$ - see front matter © 2011 Elsevier Ltd. All rights reserved.
doi:10.1016/j.jpcs.2011.08.020

Table 1
Summary of some BHJ solar cells using low molecular weight organic semiconductors.

Cell structure	Fabrication processes	V_{oc} (V)	J_{sc} (mA/cm^2)	*FF*	η (%)	Ref.
ITO/PEDOT:PSS /ZnTPP:C_{60}/PTCDA/Al	Wet	0.33	0.62	0.38	0.078	[2]
ITO/PEDOT:PSS/ethyl-TES-ADT:PCBM/CsF/Al	Wet	0.84	2.96	0.4	1	[10]
ITO/PEDOT:PSS/CuPc:PCBM/BCP/Al	Wet	0.52	1.53	0.34	0.27	[11]
ITO/PEDOT:PSS/ZnPctBu4:PCBM/BCP/Mg:Ag	Wet	0.45	0.76	0.25	0.09	[12]
ITO/PEDOT:PSS/ZnPc:C_{60}/BCP/Mg:Ag	Dry	0.44	9.3	0.43	1.7	[12]
ITO/PEDOT:PSS/Pentacene:C_{60}/BCP/Mg:Ag	Dry	0.33	4.4	0.38	0.55	[13]
ITO/C_{60} /C_{60}:ZnPc/PV-TPD/p-PV-TPD/p-ZnPc/Au[a]	Dry	0.51	8.1	0.38	1.59	[14]

[a] At room temperature.

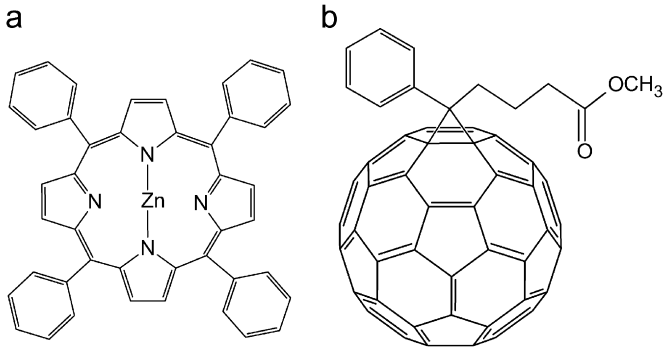

Fig. 1. Molecular structures of (a) ZnTPP and (b) PCBM.

similar to chlorophyll, are organic semiconductors having p-type nature [16]. Porphyrins have long attracted attention as potential light absorbers for photovoltaic applications because porphyrinic compounds are intimately involved in light absorption, exciton transport, primary charge separation and charge–transport processes in natural photosynthesis [17]. There have been many attempts to produce porphyrin-containing artificial donor–acceptor systems to mimic the early steps of photosynthesis, either for solar applications or as chemical energy for artificial light-driven proton pumps [18]. The main disadvantage of phythalocyanines and porphyrins is that they are not soluble in ordinary solvents and form low quality films by wet processing. To study the optoelectronic properties of porphyrins and phthalocyanines in BHJ solar cells, their soluble derivatives can be used as active materials.

In this study, we demonstrate the photovoltaic properties of simple BHJ solar cells based on a blended film of a porphyrin derivative 5,10,15,20-Tetraphenyl-21H,23H-porphine zinc (ZnTPP) and a fullerene derivative [6,6]-phenyl-C_{61} butyric acid methyl ester (PCBM) as the active layer. ZnTPP was used as a p-type semiconductor [16], and PCBM with excellent electron affinity was used as n-type. The porphyrin has a strong optical absorption in the visible spectrum [3] and was expected to form co-crystallites with PCBM [2,19]. The molecular structures of ZnTPP and PCBM are shown in Fig. 1.

2. Experimental

The fabrication of solar cells in this study was carried out in the following manner:

A hole transport layer of poly(3,4-ethylenedioxythiophene): poly(styrenesulfonate) (PEDOT:PSS) complex (Bayer Corporation) was spin-cast onto a pre-cleaned indium–tin-oxide (ITO)-coated glass slide at 1400 rpm for 78 s and then dried at 100 °C for 10 min under atmospheric conditions. PEDOT:PSS has a high electrical conductivity in the range of 400–600 S/cm and high optical transparency [20]. The blended solution was prepared by dissolving ZnTPP (Sigma–Aldrich) and PCBM (Nano C) in respective weight ratios of 1:1, 3:7, 1:9 and 0:10 for a total of 20 mg in 1 ml ortho-dichlorobenzene (o-DCB) solvent and kept stirring overnight. Thus, in each case the overall concentration of the solution was 2% wt./vol. (In one case, 3% wt./vol. solution was used, as shown in Table 2). The ZnTPP:PCBM blended solution was spin-cast on the PEDOT:PSS layer at 1200 rpm for 60 s. Deposition of each layer was followed by optical reflection and transmission measurements with a Filmetrics F20-UV thin film spectrometer system. Finally, a 70 nm thick Al electrode was deposited onto the blended layer through shadow mask by thermal evaporation under a vacuum better than 10^{-6} Torr. The deposition rate of Al was maintained at 15–20 Å/s. The active area of the solar cell was 0.12 cm^2. In some cases, thermal annealing was performed prior to Al electrode deposition as described in Table 2.

The photocurrent spectra were measured using a 300-W Xe lamp in combination with a CVI CM100 monochromator as the illumination source and a Keithley 485 picoammeter to record the short circuit currents $I_{SC}(\lambda)$. The power spectrum $P_{in}(\lambda)$ of the lamp was determined with a calibrated Si diode. Current density–voltage (*J–V*) curves were measured with a Keithley 236 source measure unit in the dark as well as under AM 1.5G simulated solar spectrum. An AM 1.5G filter (Oriel Instruments), calibrated for the 300-W Xenon arc lamp, was placed in front of the lamp to produce the simulated solar spectrum. The AM 1.5G solar spectrum was set to an intensity of 100 mW/cm^2 (1 sun) using a calibrated silicon photodiode. A schematic diagram and SEM image of cross section of the ZnTPP:PCBM 1:9 BHJ solar cell are shown in Fig. 2. Keeping in view the film fabrication technique (spin coating) and despite the uneven fracturing of amorphous glass substrate for the SEM sample preparation, the nice uniform contact between Al electrode and active layer shown in Fig. 2(b) indicates fairly smooth surface of spin coated blended layer on a rough ITO surface. The film smoothness was achieved by PEDOT:PSS layer coated on the ITO surface.

The optical density (*OD*) of the ZnTPP:PCBM blended layer was determined using Eq. (1) [21] for the reflection (*R*) and transmission (*T*) data of Fig. 3 with the subtraction of the *OD* due to the PEDOT:PSS layer. The resulting *OD* was used to determine film thickness of the active layer using Eq. (2). (Beer–Lambert's Law)

$$OD = -\log\left(\frac{T}{1-R}\right) \tag{1}$$

$$d = 2.3\frac{OD}{\alpha_{AVG}} \tag{2}$$

where d is the film thickness and α_{AVG} is the average of the absorption coefficients of ZnTPP (1.1×10^4 cm^{-1} at 510 nm) [22] and PCBM (2×10^4 cm^{-1} at 512 nm) [23] based on their weight ratio.

Table 2
Measured parameters of ITO/PEDOT:PSS/ZnTPP:PCBM /Al bulk heterojunction solar cells[a].

ZnTPP:PCBM Ratio	Concentration (%wt./vol.)	Thickness of blended layer (nm)	Annealing conditions	*RR* at ±1 V	At AM 1.5			
					V_{oc} (V)	J_{sc} (mA/cm^2)	*FF*	η (%)
1:1	2	75		42.6	0.375	0.383	0.34	0.0488
1:1	2	75	130 °C/10 min	13.91	0.422	0.208	0.3	0.0263
3:7	2	69		78.12	0.4	0.561	0.35	0.0782
3:7	2	69	100 °C /10 min	38.98	0.336	0.401	0.25	0.0338
3:7	3	119		36.17	0.48	0.166	0.19	0.0151
1:9	2	68		106.36	0.4	1.241	0.4	0.197
1:9	2	68		106.36	0.4	1.316	0.4	0.21
0:10	2	70		4.56	0.213	0.333	0.32	0.0233

[a] Solar cell devices were fabricated chronologically in the same order as listed in this Table.

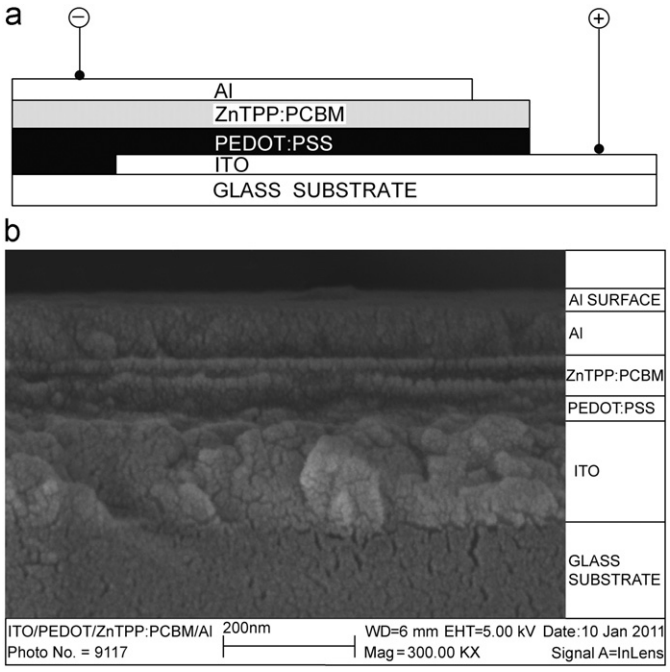

Fig. 2. Schematic diagram (a) and SEM image of cross section (b) of fabricated ZnTPP:PCBM 1:9 BHJ solar cell.

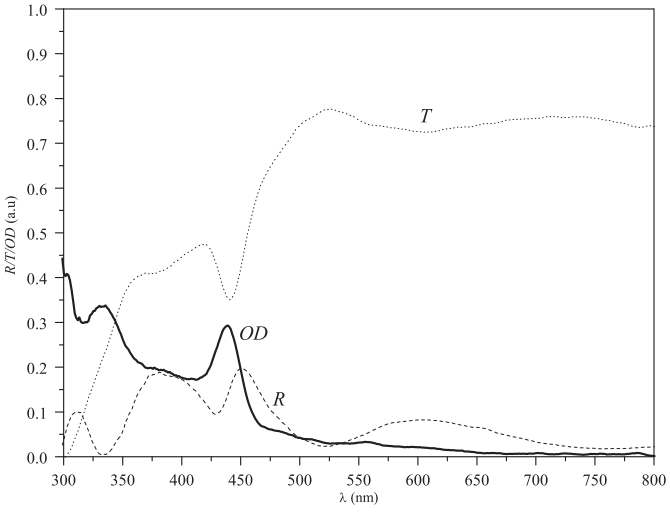

Fig. 3. Optical density (*OD*) of active layer obtained from reflection (*R*) and transmission (*T*) curves of ZnTPP:PCBM 1:9 BHJ solar cell.

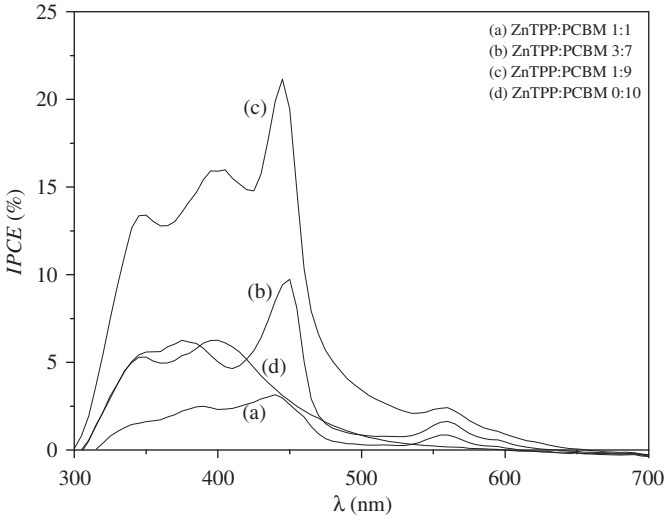

Fig. 4. Comparative IPCE spectra of ZnTPP:PCBM BHJ solar cells.

3. Results and discussions

From the photocurrent spectra $I_{SC}(\lambda)$ and lamp power spectrum P_{in} (λ) of the monochromator, incident photon to current conversion efficiency (IPCE) spectra were calculated using the following expression:

$$IPCE(\%) = \frac{1240 I_{SC}(\mathrm{A/cm^2})}{P_{in}(\mathrm{W/cm^2})\lambda(\mathrm{nm})} \times 100 \quad (3)$$

The IPCE spectra of ZnTPP:PCBM bulk heterojunction solar cells are shown in Fig. 4. The IPCE maxima occurred at 440 nm (indicating major contribution of ZnTPP) except for the 0:10 device, whose maximum (6%) was at 400 nm (indicating the absence of ZnTPP). The *J–V* characteristics of the solar cells under dark as well as under an illumination of AM 1.5G (1 sun) are shown in Fig. 5. The solar cells were illuminated through the side of the ITO substrates, and the illuminated area was 0.12 cm^2. It is seen that the *J–V* characteristics are nonlinear and asymmetrical, showing rectification behavior, i.e. the junction exhibits diode-like behavior, however, ideal diode characteristics are usually not achieved using organic semiconductors. The rectification ratio (*RR*) of forward to reverse bias current at ±1 V for each solar cell is shown in Table 2. The bulk heterojunction is a single-layer composite structure with p and n-type semiconductors, which is denoted as ZnTPP:PCBM. The measured parameters of the fabricated solar cells are listed in Table 2. The power conversion efficiency, fill factor, short-circuit current density and open-circuit

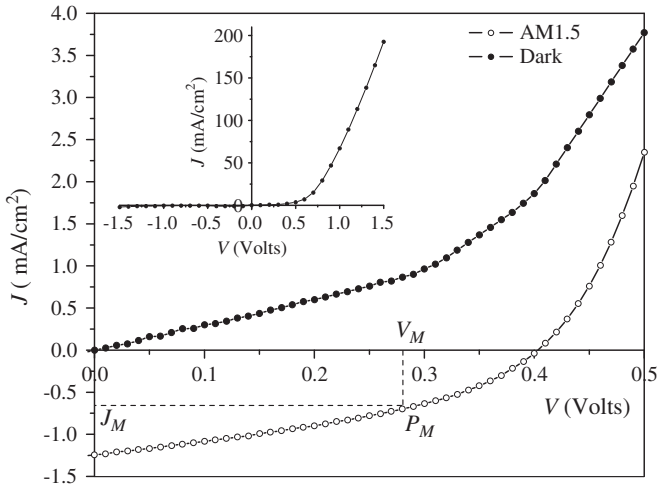

Fig. 5. *J–V* characteristics of ZnTPP:PCBM 1:9 BHJ solar cell in dark (solid circles) and under an illumination of AM 1.5G (empty circles). The inset shows dark *J–V* Characteristics.

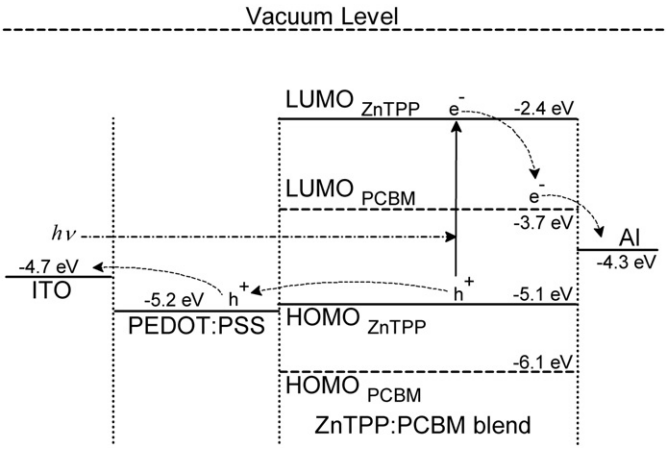

Fig. 6. Energy level diagram of ITO/PEDOT:PSS/ZnTPP:PCBM/Al BHJ solar cell.

voltage are denoted as η, *FF*, J_{SC} and V_{OC}, respectively. The fill factor is defined as the ratio of the actual maximum ($P_M = V_M I_M$) to the theoretical (not actually obtainable) power ($V_{OC} I_{SC}$), as given in Eq. (4); it therefore describes the 'squareness' of the solar cell's *J–V* characteristics. The power conversion efficiency η is the percentage of electric power converted from the power of the incident light. This is calculated as the maximum power (P_M) divided by the product of input light irradiance (*E*) and the surface area of the solar cell (*A*) as given in Eq. (5):

$$FF = \frac{V_M I_M}{V_{OC} I_{SC}} = \frac{V_M J_M}{V_{OC} J_{SC}} \quad (4)$$

$$\%\eta = \frac{V_M I_M}{EA} \times 100 = \frac{V_{OC} J_{SC} FF}{E} \times 100 \quad (5)$$

Apart from the annealed and 3% wt./vol. samples, it is seen that as the weight ratio of ZnTPP:PCBM is varied from 1:1 to 0:10, there is an increasing trend in *RR*, V_{OC}, J_{SC}, *FF* and η up to 1:9 and then these values decrease at 0:10. As shown in Table 2, the best results were obtained for the ZnTPP:PCBM 1:9 sample, whose efficiency (0.21%) of which was 36 times better than the efficiency (without exciton blocking layer) reported for ZnTPP:C_{60} 3:7 solar cells [2]. Furthermore the efficiency (0.023%) for 0:10 (PCBM only) sample was slightly lower than previously reported efficiency (0.033%) [24]. This difference may be due to the thicker PCBM film in the present case. The different D:A ratio that yields the best performance for C_{60} [2] and PCBM is attributed to the phenyl and butyric acid methylester side groups of PCBM. To check the consistency and reproducibility, ZnTPP:PCBM 1:9 solar cell was fabricated twice as shown in Table 2 and showed remarkably consistent results. Increasing the concentration to 3% wt./vol. resulted in lowering the solar cell performance as shown in Table 2, therefore 2% wt./vol. concentration was also maintained for the subsequent devices.

The energy level diagram of the ZnTPP:PCBM BHJ solar cell is shown in Fig. 6 relative to the vacuum level. The highest occupied molecular orbital (HOMO) and the lowest unoccupied molecular orbital (LUMO) levels of ZnTPP are −5.1 and −2.4 eV, respectively [25]. The HOMO and LUMO energy levels of PCBM are −6.1 and −3.7 eV, respectively [26]. Apart from better solubility in common organic solvents [9], PCBM was preferred over C_{60} as an acceptor because the energy difference between the HOMO of ZnTPP and LUMO of PCBM is 1.4eV, which is more than twice the 0.6eV difference between HOMO of ZnTPP and LUMO of C_{60} (−4.5 eV) [4]. Since the maximum value of V_{OC} is determined by the energy difference between the HOMO of the donor and LUMO of the acceptor: the ZnTPP:PCBM based solar cells demonstrated better V_{OC} than ZnTPP:C_{60} solar cells [2]. The work function of ITO, PEDOT:PSS and Al electrodes are −4.7, −5.2 and −4.3 eV, respectively. The work function corresponds to the energy between the vacuum level and the Fermi level. For metals, work function and ionization energy are the same. In moderately doped semiconductors, the Fermi level is located within the band gap. For heavily doped materials, the Fermi level shifts more or less into the conduction (case of ITO) or valence band depending on nature of doping (n or p) [27]. After absorbing a photon, ZnTPP produces an exciton, which diffuses to the nearest D–A interface and dissociates into an electron and hole. ZnTPP transfers electrons and holes to PCBM and PEDOT:PSS, respectively. PCBM transports electrons to the Al cathode while PEDOT:PSS, which acts as a hole transport and electron blocking layer, transports holes to ITO.

Porphyrins have been reported to co-crystallize with fullerenes [28], which may result in aggregation. Since the microstructure of the ZnTPP and PCBM bulk heterojunction layer is strongly dependent on the weight ratio, it is necessary to control the microstructure to form co-crystallites of ZnTPP:PCBM. In the present work, the best efficiency was obtained for the ZnTPP:PCBM device with the weight ratio of 1:9, which would be the most favorable for the co-crystallite formation [2]. The recombination of electrons and holes would occur in a bulk heterojunction layer with intermittent co-crystallite structures. If continuous co-crystallite structures are formed perpendicular to the thin films, it is expected that electron–hole recombination could be suppressed, which would lead to improvement of the conversion efficiency. It is evident from Table 2 that *RR*, V_{OC}, J_{SC}, *FF*, and η are all the largest at ZnTPP:PCBM ratio of 1:9.

It is of interest to note here that gap states or intermediate energy levels lying between the conduction and valence bands are present in the ZnTPP solid and they behave as recombination centers upon illumination [29,30]. A more recent study revealed that, first, the gap states in the porphyrin semiconductor are responsible for the NIR light absorption and second, that the electronic transitions to or from the gap states diminish the rate of recombination of electron–hole pairs via these intermediate states, leading to the enhancement of the 440 nm photocurrent [31].

In an attempt to minimize film defects, annealing of two devices (as indicated in Table 2) was performed according to the annealing cycles shown in Fig. 7. Annealing resulted in performance degradation of the devices. The reason is that annealing enhances the porphyrin aggregation already observed

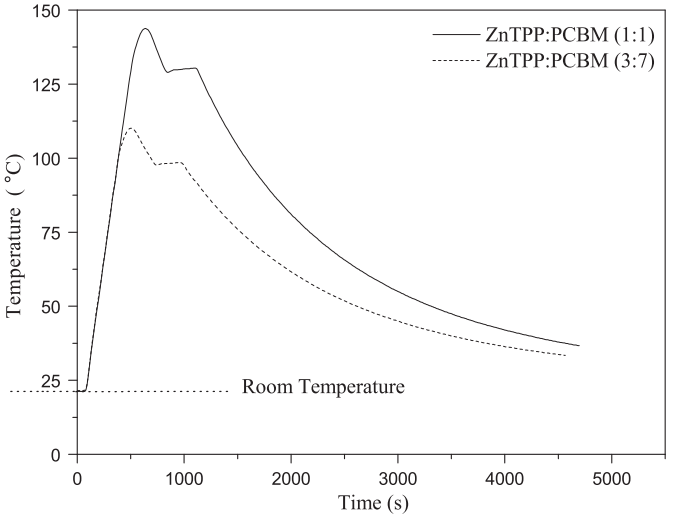

Fig. 7. Annealing temperature profiles for ZnTPP:PCBM BHJ solar cells.

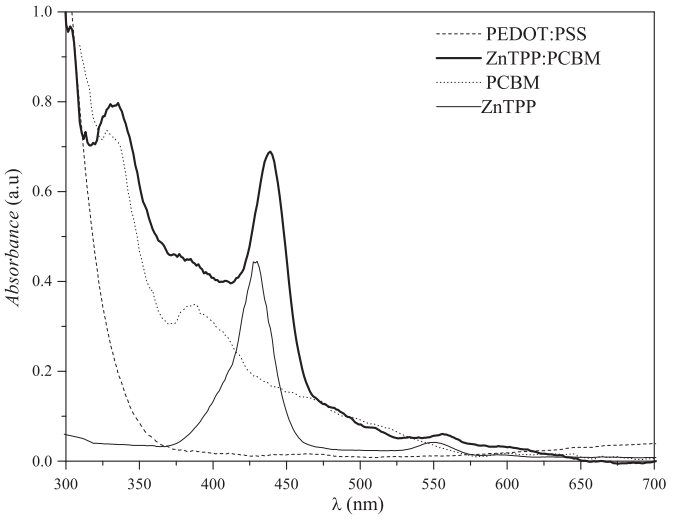

Fig. 8. Absorption spectra of ZnTPP, PCBM, and ZnTPP:PCBM (all spin-coated in o-DCB), and PEDOT:PSS.

in the room temperature spun devices [19]. Excitons generated in these larger aggregates have a lower possibility of reaching an interface and thus being converted into charge. Therefore, annealing of subsequent samples was not carried out.

The ZnTPP absorption spectrum shows the intense B band (Soret band) at 428 nm and Q band at 550 nm as shown in Fig. 8, both arising from the corresponding π–π^* transitions [32,33]. The absorption spectrum of PCBM is similar to that of C_{60}, with the absorption maximum at 327 nm and a smaller peak located at 385 nm [34]. The absorption peaks of the ZnTPP:PCBM blend at 440 nm and 333 nm are attributed to ZnTPP and PCBM, respectively. The red shifts in the absorption peaks of ZnTPP and PCBM indicate that ZnTPP forms a new complex with PCBM [35]. The PEDOT:PSS layer is mostly transparent in the visible region, however a slight increasing trend in absorption is seen at longer wavelengths.

The central part of the ZnTPP ring is occupied by a Zn ion linked to a pyrrole ring. The Zn ion accepts the lone-pair-electrons of the N atoms of the pyrrole ring, while the electrons of the Zn ion are donated to the porphyrin molecule, forming delocalized π bonds that permit the easy flow of electrons within the delocalized π system. The increasing density in the electronic levels for π–π^* transitions makes ZnTPP a relatively good electron donor [36,37]. Generally, the porphyrin/fullerene films delocalize more efficiently the excited electrons from the excited molecule as compared to pure porphyrin films on a timescale that competes effectively against loss processes, suggesting its application for efficient solar energy conversion [38].

4. Conclusions

ZnTPP:PCBM BHJ solar cells were fabricated and characterized for their electronic and optical properties. These cells showed improved V_{OC}, J_{SC}, FF and hence η as compared to ZnTPP:C_{60} [2] solar cells due to better solubility of PCBM in common organic solvents [9] and larger difference between the HOMO of ZnTPP and LUMO of PCBM (as compared to C_{60}).

Solar cells with a ZnTPP:PCBM ratio of 1:9 showed the best performance. It is seen that the donor–acceptor ratio in the fabrication of a BHJ solar cell plays a vital role in cell performance. Fabrications of BHJ solar cells using donor and acceptor co-evaporation by vacuum thermal evaporator have previously been reported [14,39,40]. The co-evaporation technique is costly, time consuming and most importantly it is very difficult to control the donor-acceptor ratios. The donor–acceptor ratio can easily be controlled or even varied (to get the optimum ratio) if fabrication of the solar cell is based on solution processing and spin-coating.

PCBM has high electron mobility ($\sim 10^{-3}$ cm^2/Vs) [41,42], as compared to the hole mobility of ZnTPP which is of the order 10^{-10} cm^2/Vs [43]. A further enhancement in efficiency could be achieved with a porphyrin derivative having a mobility on par with that of PCBM. Therefore, new donor and acceptor materials, having higher mobilities and that are soluble in common solvents for solution processing can be used to fabricate the BHJ solar cells at their optimum ratios. In the future, this will hopefully boost the performance of porphyrin and phthalocyanine BHJ solar cells fabricated by wet processing.

This work has highlighted the ease of fabrication of small molecule BHJ solar cells in respect of cost, time, simplicity and better control over D:A ratio. There is a possibility that the efficiency may be improved by the introduction of an exciton-blocking layer (EBL) such as Bathocuproine (BCP). This is plan for future work.

Acknowledgments

The authors would like to thank Department of Physics, Virginia Tech (VT), USA, and Higher Education Commission (HEC) of Pakistan for providing support and funding for this research.

References

[1] G. Yu, J. Gao, J.C. Hummelen, F. Wudl, A.J. Heeger, Science 270 (1995) 1789–1791.
[2] T. Oku, T. Noma, A. Suzuki, K. Kikuchi, S. Kikuchi, J. Phys. Chem. Solids 71 (2010) 551–555.
[3] Q. Sun, L. Dai, X. Zhou, L. Li, Q. Li, Appl. Phys. Lett. 91 (2007) 253505-1-3.
[4] C. Chu, V. Shrotriya, G. Li, Y. Yang, Appl. Phys. Lett. 88 (2006) 153504.
[5] J.J.M. Halls, K. Pichler, R.H. Friend, S.C. Moratti, A.B. Holmes, Appl. Phys. Lett. 68 (1996) 3120.
[6] D. Vacar, E.S. Maniloff, D.W. McBranch, A.J. Heeger, Phys. Rev. B 56 (1997) 4573–4577.
[7] A. Haugeneder, M. Neges, C. Kallinger, W. Spirkl, U. Lemmer, J. Feldmann, U. Scherf, E. Harth, A. Gügel, K. Müllen, Phys. Rev. B 59 (1999) 15346–15351.
[8] D.M. Guldi, N. Martin, Fullerenes: From Synthesis to Optoelectronic Properties, Kluwer Academic Publishers, Boston, 2002, p. 390.
[9] J.C. Hummelen, B.W. Knight, F. LePeq, F. Wudl, J. Yao, C.L. Wilkins, J. Org. Chem. 60 (1995) 532.
[10] M.T. Lloyd, A.C. Mayer, S. Subramanian, D.A. Mourey, D.J. Herman, A.V. Bapat, J.E. Anthony, G.G. Malliaras, J. Am. Chem. Soc. 129 (2007) 9144–9149.

[11] H. Derouiche, H.B. Miled, A.B. Mohamed, Phys. Status Solidi A 207 (2010) 479–483.
[12] T. Taima, T. Yamanari, K. Hara, K. Saito, IEICE Trans. Electron. E89–C (2006) 1771–1774.
[13] J. Sakai, T. Taima, T. Yamanari, Y. Yoshida, A. Fujii, M. Ozaki, Jpn. J. Appl. Phys. 49 (2010) 032301.
[14] S. Pfuetzner, J. Meiss, A. Petrich, M. Riede, K. Leo, Appl. Phys. Lett. 94 (2009) 253303.
[15] H. Mao, Y. Sun, H. Li, Q. Zhou, X. Zhang, J. Shen, H. Xu, Sci. China Ser. B: Chem. 41 (1998) 449–454.
[16] Y. Harima, K. Takeda, K. Yamashita, J. Phys. Chem. Solids 56 (1995) 1223–1229.
[17] C.W. Tang, A.C. Albrecht, Nature 254 (1975) 507–509.
[18] D. Gust, T.A. Moore, A.L. Moore, Acc. Chem. Res. 34 (2001) 40–48.
[19] W.J. Belcher, K.I. Wagner, P.C. Dastoor, Sol. Energy Mater. Sol. Cells 91 (2007) 447–452.
[20] Y. Yang, Morphology and Cathode Optimization for Efficient Polymer Bulk Heterojunction Solar Cells, The University of Texas, Arlington, 2009, p. 29.
[21] M. Drees, K. Premaratne, W. Graupner, J.R. Heflin, R.M. Davis, D. Marciu, M. Miller, Appl. Phys. Lett. 81 (2002) 4607–4609.
[22] J.A. Ferreira, R. Barral, J.D. Baptista, M.I.C. Ferreira, J. Lumin. 48–49 (1991) 385–390.
[23] M. Kaur, A. Gopal, R.M. Davis, J.R. Heflin, Sol. Energy Mater. Sol. Cells 93 (2009) 1779–1784.
[24] T. Yamanari, T. Taima, J. Sakai, K. Saito, Jpn. J. Appl. Phys. 47 (2008) 1230–1233.
[25] R. Ma, P. Guo, H. Cui, X. Zhang, M.K. Nazeeruddin, M. Grätzel, J. Phys. Chem. A 113 (2009) 10119–10124.
[26] P. Kumar, S.C. Jain, V. Kumar, S. Chand, R.P. Tandon, Appl. Phys. A 94 (2009) 281–286.
[27] P.S. Kireev, Semiconductor Physics, Mir Publishers, Moscow, 1978, p. 696.
[28] P.D.W. Boyd, C.A. Reed, Acc. Chem. Res. 38 (2005) 235–242.
[29] Y. Harima, M. Miyatake, K. Yamashita, Chem. Phys. Lett. 200 (1992) 263–266.
[30] Y. Harima, M. Miyatake, K. Yamashita, Chem. Phys. Lett. 229 (1994) 47–50.
[31] Y. Harima, T. Kodaka, P. Price, T. Eguchi, K. Yamashita, Thin Solid Films 307 (1997) 208–214.
[32] D.M. Cleland, K.C. Gordon, D.L. Officer, P. Wagner, P.J. Walsh, Spectrochim. Acta Part A 74 (2009) 931–935.
[33] J. Spadavecchia, R. Rella, P. Siciliano, M.G. Manera, A. Alimelli, R. Paolesse, C.D. Natale, A. D'Amico, Sensors Actuators B 115 (2006) 12–16.
[34] L. Shengli, Y. Mujie, Chem mag. 5 (2003) 49.
[35] G. Yin, D. Xu, Z. Xu, Chem. Phys. Lett. 365 (2002) 232–236.
[36] S. Uttiya, Development of Molecular Sensors based on Optical Absorption of Organic Thin Films, Mahidol University, Nakhon Pathom, Thailand, 2008, p. 45.
[37] W. Zheng, N. Shan, L. Yu, X. Wang, Dyes Pigm. 77 (2008) 153–157.
[38] P. Vilmercati, C.C. Cudia, R. Larciprete, C. Cepek, G. Zampieri, L. Sangaletti, S. Pagliara, A. Verdini, A. Cossaro, L. Floreano, A. Morgante, L. Petaccia, S. Lizzit, C. Battocchio, G. Polzonetti, A. Goldoni, Surf. Sci. 600 (2006) 4018–4023.
[39] S. Alem, A.K. Pandey, K.N.N. Unni, J.M. Nunzi, J. Vac. Sci. Technol. A 24 (2006) 645–648.
[40] T. Iwase, Y. Haga, Jpn. J. Appl. Phys. 42 (Pt1) (2003) 5330–5335.
[41] J.M. Kroon, S.C. Veenstra, L.H. Slooff, W.J.H. Verhees, M.M. Koetse, J. Sweelssen, H.F.M. Schoo, W.J.E. Beek, M.M. Wienk, R.A.J. Janssen, X. Yang, J. Loos, V.D. Michailetchi, P.W.M. Blom, J. Knol, J.C. Hummelen. Polymer Based Photovoltaics: Novel Concepts, Materials and State-of-the Art Efficiencies in proceedings of the 20th European Photovoltaic Solar Energy Conference and Exhibition, Barcelona, Spain, 2005.
[42] E.V. Hauff, V. Dyakonov, J. Parisi, Sol. Energy Mater. Sol. Cells 87 (2005) 149–156.
[43] Y. Harima, S. Furusho, Y. Kunugi, K. Yamashita, Chem. Phys. Lett. 258 (1996) 213–216.